

Optical Spectroscopy of the Central Regions of Bright Barred Spiral Galaxies

J.A. García-Barreto¹, H. Aceves², O. Kuhn³, G. Canalizo⁴, R. Carrillo¹
and
J. Franco¹

Abstract

Se presentan espectros ópticos en la banda roja de 18 galaxias espirales con barra. El estudio se enfoca a la determinación de la cinemática local y condiciones del gas ionizado en el núcleo compacto (dentro de un diámetro de 5'') y en las regiones circunucleares (dentro de un diámetro de 20''). Sólo 8 galaxias presentan emisión brillante al Este y Oeste del núcleo compacto. En otras 10, las líneas de emisión son débiles y sólo pudimos obtener un espectro promedio de la emisión central. No se detectaron líneas de emisión en las otras 8 galaxias. Se presenta una estimación de la masa dinámica en la región central de cada galaxia en base a las velocidades observadas en regiones circunucleares. En NGC 4314 y NGC 6951, que presentan emisión de H α distribuida en estructuras de anillo alrededor del núcleo compacto, se determinan los cocientes [NII] λ 6583/H α y [SII]/H α para ambos lados del anillo. La diferencia de velocidades en uno y otro lado se usa como indicativo de la velocidad de rotación del gas alrededor del núcleo de la galaxia. Las velocidades encontradas en las regiones circunucleares en NGC 4314 y NGC 6951 explican naturalmente la discrepancia que existe en la literatura sobre las velocidades de recesión reportadas. Se encuentra que los cocientes [NII] λ 6583/H α y [SII]/H α son diferentes en cada lado del anillo (un factor de ~ 2 mayor en el lado oeste) y se infiere que las condiciones físicas son diferentes. El cociente [NII] λ 6583/H α en el núcleo de NGC 6951 es un factor de 2 mayor comparado con el valor de la región

oeste. Las densidades electrónicas se han estimado de los cocientes de líneas de azufre [SII].

Optical red spectra of a set of 18 bright barred spiral galaxies are presented. The study is aimed at determining the local kinematics, and physical conditions of ionized gas in the compact nucleus (inside a diameter of 5'') and in the circumnuclear regions (inside a diameter of 20''). Only 8 galaxies showed bright emission from their east and west side of the nucleus. The spectrum of each region was analyzed separately. In other 10 galaxies the line emission was so weak that we were only able to obtain an average spectrum of the central emission. No emission was detected in the remaining 8 galaxies. An estimate of the dynamical mass is presented based on the observed velocities in the circumnuclear regions. In NGC 4314 and NGC 6951, that show H α emission distributed in circumnuclear ring structures, we determine the [NII]/H α and [SII]/H α ratios for the eastern and western regions of the rings. The velocity difference for the two sides is used to derive the rotation velocity of the gas around the compact nucleus. The ratio, [NII] λ 6583/H α , is a factor of 2 larger in the compact nucleus of NGC 6951 than in its western side. The electron gas densities have been estimated from the [SII] lines ratio.

1. Introduction

The study of emission lines in spiral galaxies has proven to be very useful in determining the distribution of ionized gas, and the physical conditions at the central regions (Burbidge & Burbidge 1960a, 1960b, 1962, 1964, 1965; Burbidge, Burbidge & Pendergast 1960; Keel 1983a,b; Kennicutt & Kent 1983; Heckman, Balick & Crane 1980; Stauffer 1982a,b; Kennicutt 1992a,b; Appenzeller & Östreicher 1988; Filippenko & Sargent 1985; Ho, Filippenko & Sargent 1995, 1997a,b; Vaceli et al. 1997).

Optical observations of barred spiral galaxies usually show the presence of symmetric structures around their center (presumably in the plane of the disk) which are referred to as *rings* (e.g. Buta 1986, Buta & Croker 1991, Buta 1995). These symmetric structures are observed at different radii in their host galaxy; some are seen as extended structures at $\approx 10 - 15$ kpc from the center, but some others are located about 4 - 5 kpc, and there are circumnuclear rings at 300 - 900 pc from the compact nucleus (e.g. Arsenault et al., 1988, Pogge 1989a, 1989b; Garcia-Barreto et al., 1991a,b, 1996; Barth et al., 1995, Genzel et al.,

¹Instituto de Astronomía, Universidad Nacional Autónoma de México, Apartado Postal 70-264, México D.F. 04510 México. tony,rene,pepe@astroscu.unam.mx

²Instituto de Astrofísica de Andalucía. Apdo. Postal 3004, Granada 18080. España. aceves@iaa.es

³Observatorio Astronómico Nacional, Instituto de Astronomía, Universidad Nacional Autónoma de México, Apartado Postal 877, Ensenada, Baja California C.P. 22100, México

⁴Institute for Astronomy, University of Hawaii, 2680 Woodlawn Drive, Honolulu, HI 96822

1995). A dynamical explanation for the origin of the structures has been sought in terms of non-symmetric perturbations to the ‘normal’ gravitational potential of spiral galaxies (Binney & Tremaine 1987). The standard model to explain the formation of circumnuclear structures requires knowledge of the angular velocity of the gas and stars (Ω_g), the epicyclic frequencies (κ), and an estimate of the angular velocity of the bar (Ω_b). In this model, it is generally assumed that the gravitational potential of the bar and Ω_b are independent of time (Binney & Tremaine 1987). Some of these galaxies have nearby neighbors and many numerical models have been carried out to examine the possible role of tidal interactions in the formation of bars and symmetric structures (e.g. Noguchi 1988, Friedli & Benz 1993).

Previous spectra of Shapley Ames Galaxies (Filippenko & Sargent 1985, Ho, Filippenko & Sargent 1995, Ho, Filippenko & Sargent 1997a, Ho, Filippenko & Sargent 1997b) represents the emission of the innermost $2'' \times 7''$ or $r \leq 200$ pc. Here we present new optical spectroscopic observations of the central regions of 18 barred galaxies using a long slit. Our main purpose is to provide local velocities and line ratios from the emission lines of [NII], $H\alpha$, and [SII], for both the nucleus and the circumnuclear regions. We have tried to obtain spectra of the compact nucleus and from the immediate surroundings separately (in the east and west directions since the slit was oriented at $PA \sim 90^\circ$ E of N) by adding only the corresponding pixels in the slit. A clear example of this is in NGC 6951, where the spatial distribution of $H\alpha$ shows the compact nucleus in addition to a circumnuclear ring. NGC 4314 also presents the circumnuclear ring in $H\alpha$, but no emission from the compact nucleus is detected in this case. In other six galaxies the spatial distribution of the $H\alpha$ emission is more diffuse. In 10 galaxies we were only able to obtain a spectrum of the central emission: compact nucleus and weak (if present at all) extranuclear emission.

The present work is divided as follows. In section 2, the selection criteria for the set of galaxies observed are established, and the observations are described. In section 3, our results are presented and discussed. In section 4, a brief summary is presented.

2. Sample and Observations

The galaxies studied here are part of an ongoing study of barred galaxies (see García-Barreto et al.

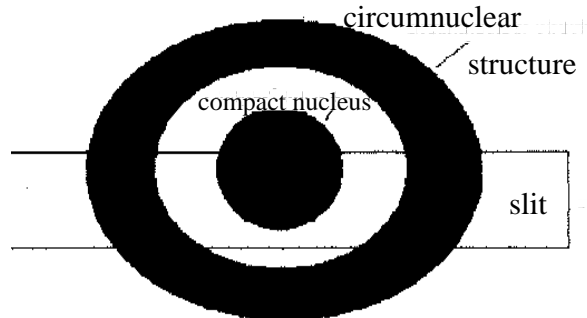


Fig. 1.— Sketch (not to scale) of the slit position relative to a circumnuclear region in the central region of a given galaxy. The slit in all cases positioned at PA 90° or east - west. Final length of slit was 59 pixels long or $43''$, and 10 pixels wide or $7''.3$.

1993,1996), and they were chosen using the following criteria: 1) bright barred galaxies in the Shapley Ames Catalog (first or second edition Sandage & Tammann 1987), 2) with declinations within a range accessible from San Pedro Mártir, $-41^\circ \leq \delta \leq +70^\circ$, and 3) with IRAS colors characteristic of star-forming galaxies according to Helou (1986; with $\log(f(12)/f(25)) \leq -0.15$ and $\log(f(60)/f(100)) \leq -0.1$) or equivalently, an IRAS dust temperature $T_d \geq 25$ K. The characteristics of each galaxy such as distance, IRAS fluxes, radio continuum fluxes, dust temperature, blue luminosity, HI mass, X-Ray luminosity and inclination, are summarized in García-Barreto et al. (1993,1996). The purpose of the observations was to determine the physical conditions (velocities and line ratios) from the innermost central regions (circumnuclear structure and compact nucleus). The slit length and width were selected accordingly. Table 1 lists the systemic velocities from optical, HI and CO observations taken from the literature, as well as whether a given galaxy shows $H\alpha$ emission from either the compact nuclear region (innermost $5''$ in diameter) and or circumnuclear regions (innermost $20''$ in diameter) (ie. Pogge 1989a, Pogge 1989b, Garcia-Barreto et al., 1996).

The optical observations were performed at the Observatorio Astronómico Nacional in San Pedro Mártir, Baja California, México, on 1993, May 28, 29, 30, 31 and June 1, using the 2.12m telescope $f/7.5$ equipped with a 1024×1024 Thompson CCD detector coupled to a Boller & Chivens spectrograph with 600 grooves per mm at a grating angle of 13° . The central wavelength was chosen in the red part of the

TABLE 1
OBSERVED GALAXIES.

Galaxy ^a	Optical ^b	HI ^c	CO ^d	i^e	PA _{bar} ^e	CiNE ^f	CoNE ^f
3504	1535±19	1538	1550	35	145	N	Y
4123	1325±10	1327		39	105	N	Y
4314	883±85	982	985	30	145	Y	N
4477	1263±75	1263		26	15	?	?
4691	1123±13	1119	1124	32	85	Y?	Y?
5135	4157±35	4157		67	125	Y	Y
5347	2373±12	2386		37	100	Y	Y
5383	2260±3	2264		40	130	Y?	Y
5430	2875±90	2960	2981		145	N	Y
5534	2633±10	2633			80	N	Y
5597	2624±66				55	Y	Y
5691	1876±50			34	90	Y?	Y
5728	2970±40	2780		65	35	Y	Y?
5757	2771±58			32	165	Y	N
5915	2273±14	2274		42	90	Y?	Y?
6239	938±12	931		67	115	N	Y?
6907	3155±80	3139			45	Y	Y
6951	1425±10	1426	1464	28	85	Y	Y

^aNGC catalog numbers

^bSystemic Velocity in km s^{-1} from Revised Shapley Ames Catalog, (Sandage & Tammann 1987)

^cSystemic Velocity in km s^{-1} from Huchtmeier & Richter (1989),except for NGC 4314 which we used the value observed by Garcia-Barreto, Downes & Huchtmeier 1994

^dSystemic Velocity in km s^{-1} from Young et al., (1995) for most of the galaxies except for NGC 4314 taken from Garcia-Barreto et al., (1991b)

^eInclination of the galaxy's disk with respect to the plane of the sky; position angle of the stellar bar measured East of North taken from Tully (1988) or Huchtmeier & Richter (1989)

^fObserved spatial H α + [NII] emission : Circumnuclear or extranuclear (innermost 20'') (CiNE); compact nucleus (innermost 5'')(CoNE) from Pogge (1989a,b), Garcia-Barreto et al., (1996)

TABLE 2
EMISSION LINES OF GALAXIES WITH CIRCUMNUCLEAR REGIONS.

Galaxy	Region	Pix ^a	[NII] ^b	[NII]/H α	H α ^b	FWHM ^c	H α Flux ^d	[NII] ^b	[NII]/H α	[SII] ^b	[SII]/H α	[SII] ^b	[SII]/H α
3504	E	6	1385	0.17	1383	215	12.0	1391	0.53	1403	0.13	1413	0.12
	W	3	1475	0.17	1470	237	9.7	1476	0.57	1498	0.13	1489	0.13
	N	6	1430	0.17	1422	253	11.0	1434	0.60	1440	0.12	1445	0.13
4314	E	12	935	0.13	868	237	1.6	853	0.45	903	0.09	913	0.18
	W	11	997	0.21	983	224	1.0	945	0.85	891	0.18	938	0.25
4691	E	9	1017	≤ 0.01	1050	151	2.4	1062	0.38	1025	0.08	1066	0.07
	W	6	1038	0.07	1055	210	4.8	1059	0.41	1039	0.10	1073	0.09
	W ^e	11			635	1475	38.9						
5135	N	6	1068	0.11	1068	207	16.4	1081	0.42	1091	0.09	1089	0.09
	E	5	3996	0.15	3965	279	1.1	3961	0.77	3783	0.21	3954	0.16
	W	4	4021	0.29	3988	247	7.1	3896	0.89	3995	0.17	4024	0.19
5383	N	4	3970	0.25	3966	334	19.9	3954	0.76	3962	0.15	3991	0.13
	E	14	2589	0.10	2453	224	2.3	2403	0.13	2433	0.14	2829	0.10
5534	W	13	2240	0.06	2257	219	5.4	2265	0.25	2271	0.10	2202	0.08
	N	5			2376	56	0.8	2336	0.43				
	E	13	2487	0.14	2477	233	11.1	2483	0.45	2497	0.15	2504	0.14
5915	W	14	2440	0.05	2502	173	0.9	2510	0.27	2531	0.11	2651	0.14
	E	18	2192	0.09	2207	196	1.5	2216	0.26	2151	0.07	2348	0.09
6951	W	12	2094	0.16	2061	201	1.6	2091	0.41	2061	0.18	2097	0.14
	N	8	2148	0.18	2133	259	2.9	2147	0.49	2127	0.21	2185	0.14
	E	6	1517	0.15	1491	247	1.1	1485	0.48	1652	0.09	1607	0.10
6951	W	4	1399	0.28	1348	251	1.1	1371	0.93	1215	0.08	1228	0.09
	N	7	1389	0.85	1428	285	0.8	1397	1.99	1423	0.32	1398	0.36

^aPixels added in slit for each region to produce the final spectra

^bObserved heliocentric velocity centroids in km s⁻¹. The velocity centroid uncertainties amount to about 25 km s⁻¹ as a result of wavelength calibration and gaussian fitting. Columns 4 and 5 correspond to [NII] λ 6548.1 Å, columns 9 and 10 to [NII] λ 6583.4 Å, columns 11 and 12 to [SII] λ 6716.4 Å, and columns 13 and 14 to [SII] λ 6730.8 Å

^cH α full width at half maximum, in km s⁻¹, after deconvolution with an instrumental response (FWHM_{inst} \sim 3.23 \pm 0.1 Å = 145 \pm 5 km s⁻¹).

^dH α flux in units of 10⁻¹⁴ ergs s⁻¹ cm⁻²

^eBroadline from a western spectrum 12'' away from the spectrum of narrow lines (Garcia-Barreto et al., 1995)

TABLE 3
EMISSION LINES FROM GALAXIES WITH ONLY A CENTRAL SPECTRUM.

Galaxy	Region	Pix ^a	[NII] ^b	[NII]/H α	H α ^b	FWHM ^c	H α Flux ^d	[NII] ^a	[NII]/H α	[SII] ^a	[SII]/H α	[SII] ^a	[SII]/H α
4123	N	12	1211	0.15	1193	251	11.3	1196	0.51	1239	0.14	1215	0.12
4477	N	13	1355	0.70	1373	205	0.8	1375	2.37	1410	0.39	1404	0.57
5347	N	10	2349	0.25	2325	384	2.1	2291	0.71	2349	0.34	2329	0.35
5430	N	10	3073	0.19	3055	320	5.4	3051	0.54	3070	0.14	3101	0.11
5597	N	17	2491	0.15	2452	269	19.0	2467	0.44	2493	0.10	2605	0.06
5691	N	13			1733	164	0.6			1745	0.19	1831	0.25
5728	N	14	2852	0.45	2870	507	6.2	2850	1.39	2857	0.40	2865	0.32
5757	N	5	2517	0.14	2505	283	15.9	2516	0.45	2530	0.11	2533	0.11
6239	N	20			1060	132	4.8	1061	0.12	1061	0.10	1072	0.05
6907	N	18	2968	0.16	2940	347	9.2	2947	0.45	2925	0.09	3002	0.07

^aPixels added in slit for central region to produce the final spectrum

^bObserved heliocentric velocity centroids in km s⁻¹. The velocity centroid uncertainties amount to about 25 km s⁻¹ as a result of wavelength calibration and gaussian fitting. Columns 4 and 5 correspond to [NII] λ 6548.1 Å, columns 9 and 10 to [NII] λ 6583.4 Å, columns 11 and 12 to [SII] λ 6716.4 Å, and columns 13 and 14 to [SII] λ 6730.8 Å

^cH α full width at half maximum, in km s⁻¹, after deconvolution with an instrumental response (FWHM_{inst} \sim 3.23 \pm 0.1 Å = 145 \pm 5 km s⁻¹).

^dH α flux in units of 10⁻¹⁴ ergs s⁻¹ cm⁻²

spectrum in order to include the [N II], H α and [S II] lines. The detector scale gives a 1.6 \AA pixel $^{-1}$ spectral resolution and a spatial resolution of 0".73 pixel $^{-1}$ in the spectroscopic mode. The original slit length was 80 pixels long (or 58") by 10 pixels (or 7.3") wide positioned at P.A. $\sim 90^\circ$ (E of N), that is, East – West. In order to avoid edge effects, we discarded in the final analysis altogether the outer 21 pixels from the slit length and thus the final slit length was only 59 pixels or 43". Only emission from about 19" on each side of a central region of a galaxy was observed assuming that the compact nucleus was positioned in the middle of the slit covering the innermost 7 pixels.

The slit was positioned on the brightest optical region of each galaxy, at the declination corresponding to the compact nucleus. Figure 1 shows a sketch of the relative position of the slit with respect to a circumnuclear structure in the innermost central region of a galaxy. Our final analysis showed that in some galaxies the slit was off nucleus by a few arcseconds.

The on source time was 1200s for all the galaxies in the list (except for NGC 5915 which was observed for only 900s). Each galaxy observation was followed by a 1 second exposure of a tungsten lamp. Dome flats taken with the same instrumental setup were used to flatten each galaxy spectrum. The data were bias-subtracted and flat-fielded using the NOAO IRAF software. The sky was subtracted with the IRAF task background using for each galaxy the apertures without any line emission (usually on the edges of the slit).

Not all the galaxies had emission away from the central pixels which correspond to the nucleus. Our original list of galaxies was 26, but we only detected emission lines in the spectra of 18 of them. Eight out of 18 showed emission from the east and west side of the central regions, and 6 out of 8 showed emission from their compact nuclear region as well. In the end we extracted three different final spectra from each of the eight galaxies. In order to extract the final spectra we used the IRAF task `apall` where we co-added the pixels that correspond to each region. The numbers of pixels that were co-added to create each spectrum are given in the third column of Table 2. In none of the galaxies did we detect emission from the complete disk and thus no rotation curve could have been produced. Figures 2, 3, 4, 5, 6, 7, 8, 9 shows the spectra of the eight galaxies from their eastern and western circumnuclear regions. Ten galaxies did not show any bright emission away from their central pixels and a final spectrum for each of them was obtained after

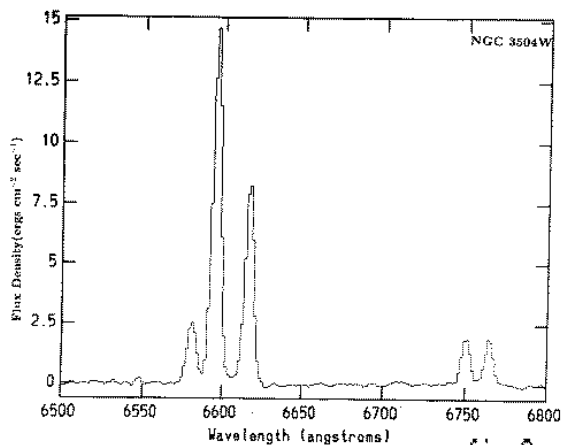
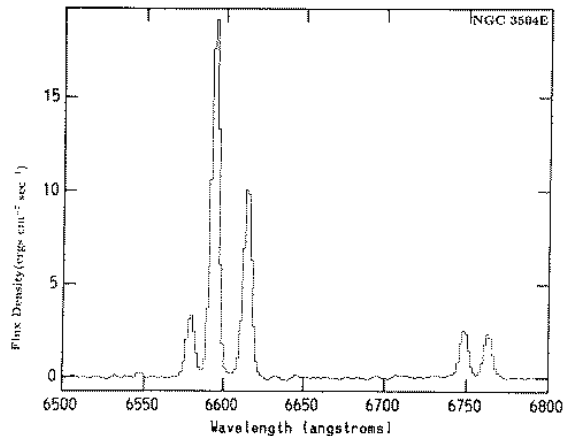


fig 2a

Fig. 2.— Spectra from the eastern (upper) and western (lower) circumnuclear regions of bright barred spiral galaxies calibrated in wavelength, sky, flux and redshift. The position of the slit was always at the P.A. 90° . Flux units are 10^{-15} ergs s $^{-1}$ cm $^{-2}$ \AA^{-1} . Here for NGC 3504.

adding the central 5 to 20 pixels.

The task “`splot`” was used to measure the strengths, central wavelengths, widths, and fluxes of the emission lines. The central wavelengths, widths and fluxes of emission lines were estimated by fitting gaussian curves with the IRAF task `splot`. For this purpose we fitted multiple curves in order to account for blended broad lines and when possible corroborated the values by fitting individual lines. The uncertainty for the velocity centroids of the emission lines amounts

TABLE 4
EAST-WEST VELOCITY DIFFERENCES AND LINE RATIOS.

Galaxy	ΔV_{e-n}^a	ΔV_{e-w}^a	ΔV_{n-w}^a	[SII]/[SII] ^b	$n_e \text{ cm}^{-3c}$
3504	-39	-39	0	1.0	$\sim 1000 \pm 600$
4314		-121		0.6	$\sim 4500 \pm 1000$
4691	-20	-10	10	1.1	$\sim 750 \pm 250$
5135	7	-19	-26	1.3	$\sim 400 \pm 200$
5383	75	230	155	1.2	$\sim 500 \pm 200$
5534		-22		1.4	< 100
5915	68	143	75	1.0	$\sim 1000 \pm 600$
6951	59	138	79	0.9	$\sim 1600 \pm 600$

^aH α velocity differences: e-n means east minus nucleus; e-w means east minus west and n-w means nucleus minus west. All velocities are taken from tables 2, 3 and 4.

^bSulfur line ratio [SII] λ 6716.4 Å over [SII] λ 6730.8 Å

^cApproximate electron densities (Osterbrock 1989)

TABLE 5
LINE RATIOS.

Galaxy	[SII]/[SII] ^a	$n_e \text{ cm}^{-3b}$
4123	1.1	$\sim 750 \pm 250$
4477	0.7	$\sim 3500 \pm 750$
5347	1.0	$\sim 1200 \pm 600$
5430	1.2	$\sim 500 \pm 200$
5597	1.5	≤ 100
5691	0.9	$\sim 1600 \pm 600$
5728	1.2	$\sim 500 \pm 200$
5757	1.0	$\sim 1200 \pm 600$
6239	~ 2.0	< 100
6907	~ 1.3	$\sim 300 \pm 200$

^aSulfur line ratio [SII] λ 6716.4 Å over [SII] λ 6730.8 Å

^bApproximate electron densities (Osterbrock 1989)

TABLE 6
ESTIMATES OF DYNAMICAL CENTRAL MASSES.

Galaxy	Distance ^a	R(pc)	$V = V_{obs}/\sin(i)$ ^b	M_{dyn} ^c
3504	26.5	560	83	$8.5 \cdot 10^8$
4314	10.0	390	115	$1 \cdot 10^9$
4691	22.5	480	34	$1.3 \cdot 10^8$
5135	53.2	755	24	$1 \cdot 10^8$
5383	37.8	1740	185	$1.4 \cdot 10^{10}$
5534	35.0	1730	25	$2.4 \cdot 10^8$
5915	33.7	1430	108	$4 \cdot 10^9$
6951	24.1	595	170	$4 \cdot 10^9$

^ain Mpc from Tully (1988).

^bTrue velocity difference, in km s^{-1} , between the nucleus and the west (east) side in (NGC 4691), NGC 5135, NGC 5383, NGC 5915 and NGC 6951. True velocity half difference between the east and west sides in NGC 4314 and in NGC 5534, for which we assumed an inclination of 30° .

^cDynamical mass of each galaxy inside a radius R, in units of solar masses: $M_{dyn} = 233.7 R(\text{pc}) V^2(\text{km s}^{-1})^2$

to about 25 km s^{-1} as a result of wavelength calibration and gaussian fitting. The instrumental spectral resolution was estimated by calculating the full width at half maximum of emission lines of a lamp at different wavelengths across the band. Our estimated value is $FWHM_{inst} \sim 3.23 \pm 0.1 \text{ \AA}$ or about $145 \pm 5 \text{ km s}^{-1}$. The tabulated line widths were corrected for instrumental resolution by subtracting the instrumental width in quadratures from the observed width: $FWHM_{real}^2 = FWHM_{obs}^2 - FWHM_{inst}^2$.

3. Results and Discussion

In this section we present the results of our observations: first, we provide the estimates of central masses calculated from the observed velocities, assuming that the ionized gas rotates on circular orbits around the compact nucleus and lies on the plane of each galaxy's disk. The velocities may also be useful in deriving the properties of resonances using density wave theory and theory of orbits in order to associate circumnuclear structures with Inner Lindblad Resonances (see Binney & Tremaine 1987 and Contopoulos & Grosbøl 1989). The spatial distribution of $H\alpha + [\text{NII}]$ of these barred galaxies, except for NGC 5383, has been reported by Pogge 1989a, Pogge 1989b and Garcia-Barreto et al., 1996. Then, the line ratios and electron densities can be derived.

3.1. Velocities and Inner Masses

Table 2 lists the heliocentric velocities, in km s^{-1} , for $[\text{NII}]\lambda 6548.1$, $H\alpha \lambda 6562.8$, $[\text{NII}]\lambda 6583.4$ and $[\text{SII}]\lambda 6716.4$ and $\lambda 6730.8$ lines from the 8 galaxies we where were able to isolate the emission from the eastern and western sides. Table 3 lists the heliocentric velocities for other 10 galaxies with no emission away from the central pixels in our slit.

Our observations indicate that the different systemic velocities reported in the literature for NGC 4314 ($v_{sys} = 883 \text{ km s}^{-1}$ [Sandage & Tammann 1987]; $v_{sys} = 1004 \text{ km s}^{-1}$ [Smith et al. 1987; Strauss et al. 1992]) are most likely the result of their position of the slit relative to the circumnuclear structure. The velocities agree with the observed velocities for the eastern and western regions of the circumnuclear structure (see Table 2). Our optical velocities are somewhat smaller than the velocities obtained from CO lines. In particular, the eastern CO emission peaks at around $v_{east} \approx 920 \text{ km s}^{-1}$ and the western CO emission peaks at around $v_{west} \approx 1030 \text{ km s}^{-1}$ (Benedict, Smith & Kenney 1996). The differences between optical and CO lines may be the result of hydrodynamic processes at play, e.g. molecular outflows, supernovae events, etc., that may produce a different velocity for the molecular and atomic components.

In NGC 5430, we only detected a velocity of $v \approx 3065 \text{ km s}^{-1}$, which is quite different from the re-

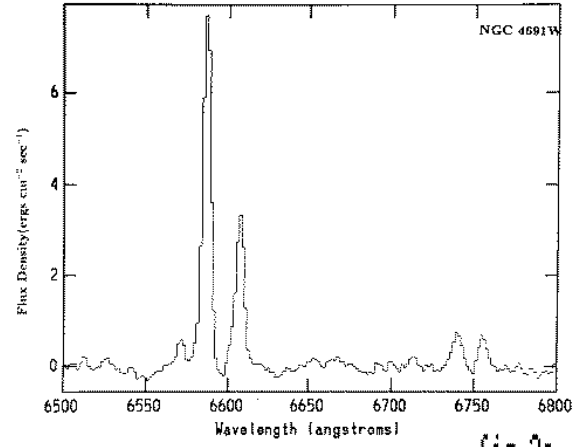
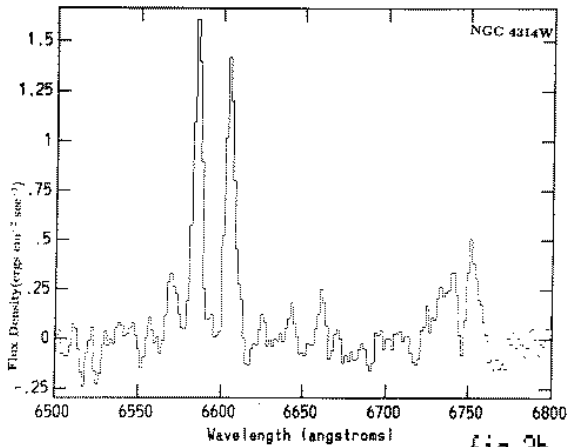
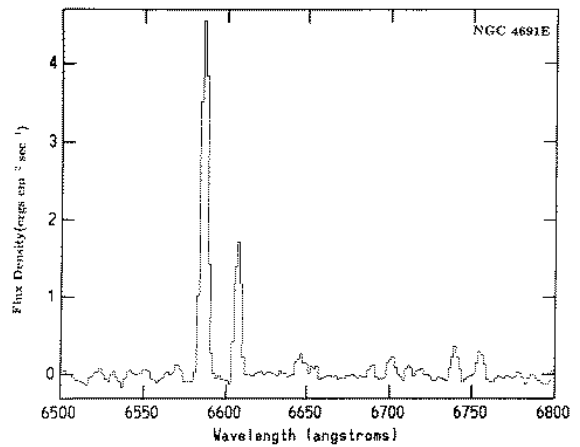
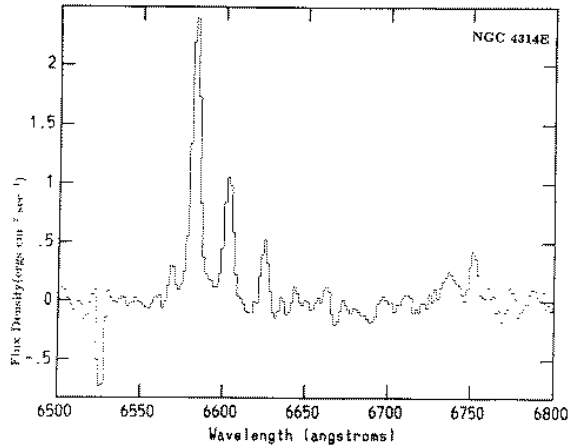


fig 2b

fig 2c

Fig. 3.— As in Fig. 2, but for NGC 4314.

Fig. 4.— As in Fig. 2, but for NGC 4691.

ported systemic optical velocity of $v_{sys} = 2875 \text{ km s}^{-1}$. On the other hand, the CO lines have $v_{NE} \approx 2893 \text{ km s}^{-1}$ and $v_{SW} \approx 3069 \text{ km s}^{-1}$ (Contini et al., 1997). This leads us to conclude that our spectrum only showed the emission from the southwestern (SW) blob, and that the reported systemic velocity is probably better associated to the NE blob.

Our velocities for NGC 4691 and NGC 6951 are in agreement with the velocities reported by Wiklind, Henkel & Sage (1993) and by Boer & Schulz (1993). The optical velocities for NGC 3504 differ by $\approx 100 \text{ km s}^{-1}$ from the CO velocities. This discrepancy is likely the result of positioning the slit off the nucleus (e.g. Kenney et al., 1992). Table 4 lists the velocity differences for the galaxies observed.

We estimate the dynamical mass interior to the rings of ionized matter. Assuming that most of the mass interior to these rings is homogeneously distributed inside a radius R , the dynamical mass may be estimated from $M_{dyn}(M_{\odot}) = 233.7 R(\text{pc}) V_{true}^2 (\text{km s}^{-1})^2$, where $V_{true} = V_{obs} / \sin(i)$, with V_{obs} the observed velocity and i is the inclination angle of the circumnuclear structure with respect to the plane of the sky. We are assuming, not necessarily being correct, that the circumnuclear structure is on the plane of a given galaxy and its inclination is the same as the inclination of the galaxy disk. This assumption is based primarily on the idea that circumnuclear structures are at distances of about 300 pc up to 1 kpc from

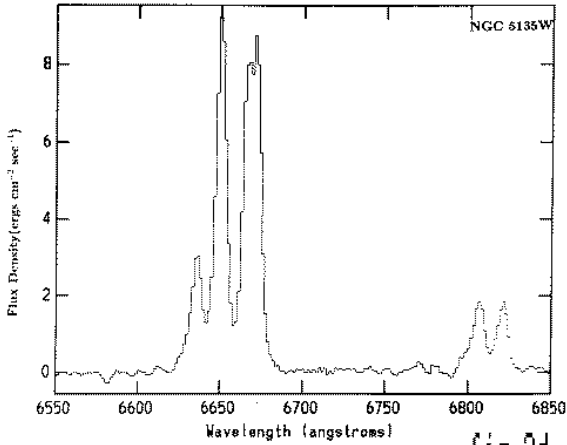
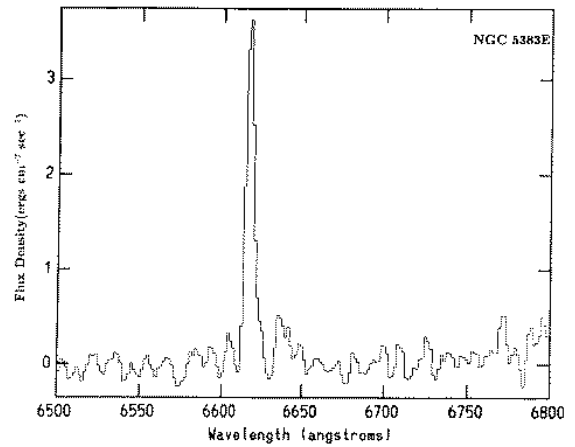
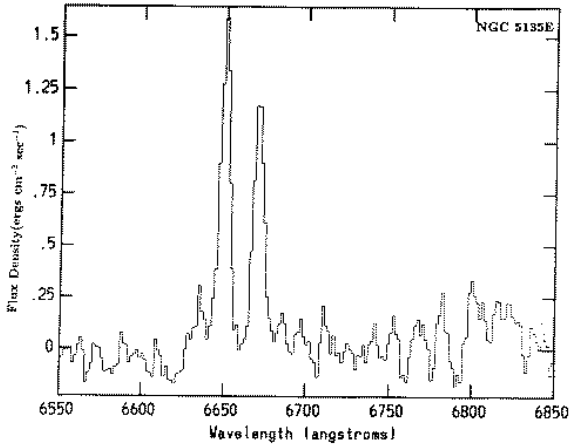


fig 2d

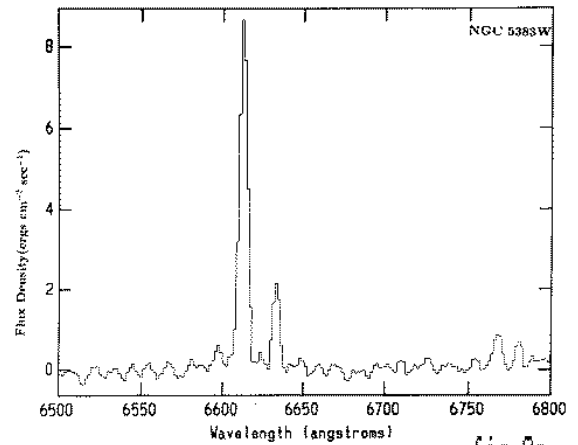


fig 2e

Fig. 5.— As in Fig. 2, but for NGC 5135.

Fig. 6.— As in Fig. 2, but for NGC 5383.

the compact nucleus and such a large structure would be unstable if being inclined with respect to the plane of the disk. In addition, we are implicitly assuming circular orbits for the gas in the rings, which might not be true especially in the presence of a pronounced bar.

Table 6 gives the estimated dynamical masses, M_{dyn} , assuming as we said before that the ionized gas in circumnuclear regions lies in the plane of the galaxy's disk and that they follow circular orbits as a response to a central axisymmetric gravitational potential. As mentioned earlier if circumnuclear structures (ie. rings) are to be explained as Inner Lindblad Resonances, more observations are needed in order

to have the complete radial velocity field (rotation curves) and to compute epicyclic frequencies, $\kappa(r)$. We estimate an error of about a factor of two on the masses presented in Table 6.

3.2. Line Ratios and Electron Densities

3.2.1. $[NII]/H\alpha$ ratio

Burbidge & Burbidge (1962) showed that the regions in external galaxies with $H\alpha$ and $[NII]$ emission lines, and a line intensity ratio of $[NII]\lambda 6583/H\alpha \sim 0.33$, have a degree of excitation that is similar to the extended HII regions in our own galaxy. They also pointed out that the observed ratio is larger than 1

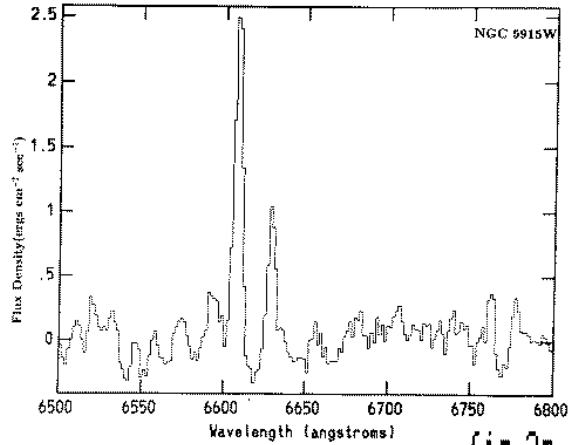
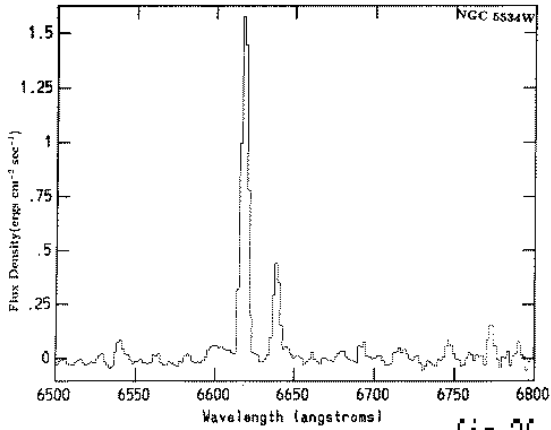
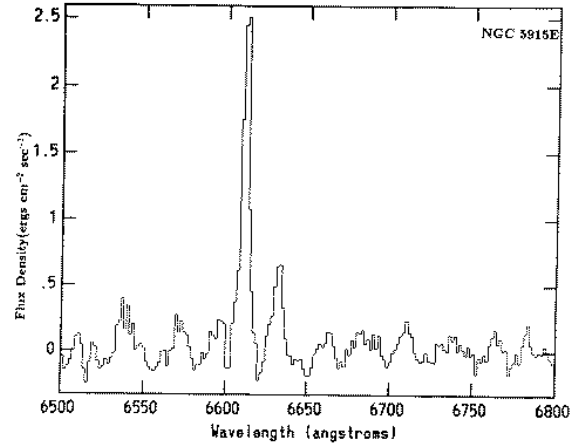
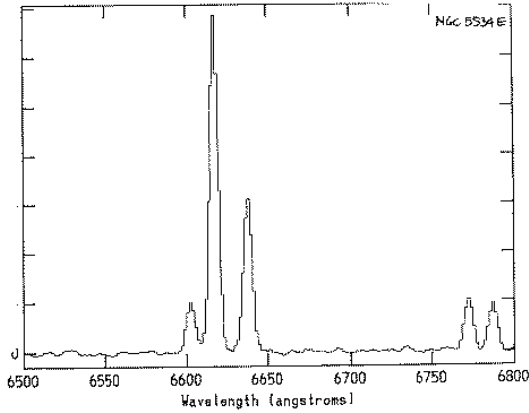


fig 2f

fig 2g

Fig. 7.— As in Fig. 2, but for NGC 5534.

Fig. 8.— As in Fig. 2, but for NGC 5915.

in the nucleus of some galaxies. More recent observations of several emission lines, with better sensitivity and spectral coverage, have been used to determine the excitation mechanisms in different objects (Baldwin, Phillips & Terlevich 1981, Osterbrock 1989). In particular, the emission lines used are: $[\text{NeV}]\lambda 3426 \text{ \AA}$, $[\text{OII}]\lambda 3727 \text{ \AA}$, $\text{H}\beta \lambda 4861 \text{ \AA}$, $\text{HeII} \lambda 4686 \text{ \AA}$, $[\text{OIII}]\lambda 5007 \text{ \AA}$, $[\text{OI}]\lambda 6300 \text{ \AA}$, $\text{H}\alpha \lambda 6563 \text{ \AA}$, $[\text{NII}]\lambda 6584 \text{ \AA}$. Depending on the line ratios, the excitation mechanisms for the line-emitting gas could be: a) photoionization by OB stars, b) photoionization by a power-law continuum source, c) collisional ionization from shock waves, and d) a combination of the above.

Actually, the nuclear regions are usually excited by a power-law source but the circumnuclear rings

are excited by UV radiation from recently formed stars. Recent spectroscopic surveys of spiral galaxies show low-ionization emission, suggesting that a flat-spectrum (power law) radiation field photoionizes the nuclear gas (Keel 1983a,b,c; Kennicutt & Kent 1983, Filippenko & Sargent 1985; Ho, Filippenko & Sargent 1995, 1997a,b; Ho et al. 1997). In the nucleus of Seyfert galaxies the same mechanism seems to operate and high-ionization emission iron lines are found from the central regions, such as: $[\text{Fe VII}]\lambda 5721 \text{ \AA}$, $[\text{Fe VII}]\lambda 6087 \text{ \AA}$, $[\text{Fe X}]\lambda 6374 \text{ \AA}$ and $[\text{Fe XIV}]\lambda 5303 \text{ \AA}$ (Appenzeller & Östreicher 1988). In contrast, several observations support the idea that circumnuclear rings are regions of massive OB star formation: e.g., those with bright $\text{H}\alpha$ emission, 10μ

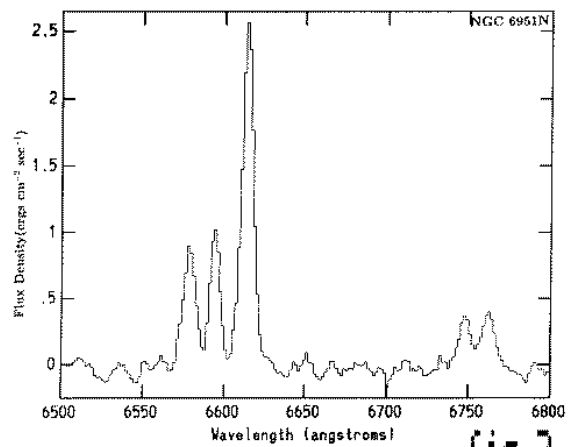
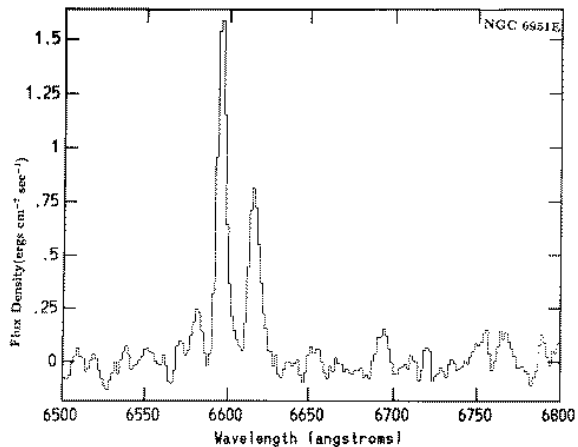


fig 3

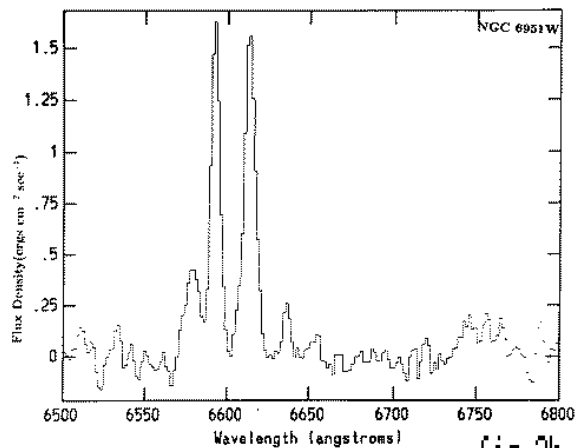


fig 2h

Fig. 9.— As in Fig. 2, but for NGC 6951.

emission, radio continuum emission, and CO mm line emission (e.g. Hummel, van der Hulst & Keel 1987, Garcia-Barreto et al., 1991a, Garcia-Barreto et al., 1991b, Kenney et al., 1992, Telesco, Dressel & Wolstencroft 1993, Vila-Vilaró et al. 1995, Benedict, Smith & Kenney 1996, Contini et al., 1997). This is in line with the expectations from galactic dynamics, where large accumulations of material can occur at regions near Lindblad resonances, hence, providing suitable conditions for triggering the formation of stars. Our results corroborate these views, and we find that the photonizing agents for the nuclear gas and the circumnuclear rings are of different nature.

The line ratios $[\text{NII}]/\text{H}\alpha$ and $[\text{SII}]/\text{H}\alpha$ were computed separately for the eastern and western regions

Fig. 10.— Spectrum from the compact nucleus in the barred galaxy NGC 6951 calibrated in wavelength, sky, flux and redshift. Notice that the $\text{H}\alpha$ intensity is much lower than the $[\text{NII}]\lambda 6583$. Flux units are $10^{-15} \text{ ergs s}^{-1} \text{ cm}^{-2} \text{ \AA}^{-1}$.

for all galaxies with circumnuclear structures. The $[\text{NII}]\lambda 6548/\text{H}\alpha$ ratio is on average ~ 0.12 in the eastern side, ~ 0.16 in the western side (Table 2). The ratio is ~ 0.25 for galaxies without extranuclear emission (Table 3). The $[\text{NII}]\lambda 6583/\text{H}\alpha$ ratio is on the average ~ 0.43 in the eastern side and ~ 0.58 in the western side. The average ratio is ~ 0.78 for galaxies presenting spectra from their central regions without circumnuclear structures. The values found are in agreement with the values found in other barred galaxies like NGC 1097 (Phillips et al., 1984).

In the case of NGC 4314 and NGC 6951, with clear circumnuclear rings, the line ratio was found different from each side of the ring. The $[\text{NII}]\lambda 6583/\text{H}\alpha$ ratios in NGC 4314 are 0.45 and 0.85 while in NGC 6951 they are 0.48 and 0.93 from their eastern and western circumnuclear regions, respectively. These values suggest different intrinsic physical conditions as a result of local star formation and evolution in each side of the ring. We believe that the ratio of $[\text{NII}]\lambda 6583/\text{H}\alpha$ of 1.01 quoted by Ho, Filippenko & Sargent 1997b for NGC 4314 represents the ratio from the western side of the circumnuclear ring and not necessarily from the compact nucleus since images suggest that there is no $\text{H}\alpha$ emission from the compact nucleus (Pogge 1989a, Garcia-Barreto et al., 1996). Additionally, the ratio $[\text{NII}]\lambda 6583/\text{H}\alpha$ from the compact

nucleus of NGC 6951 is about 2, in agreement with previous values reported (Ho, Filippenko & Sargent 1997b). Figure 10 shows the spectrum corresponding to the compact nucleus of NGC 6951. NGC 4477 and NGC 5728 also show a ratio of $[\text{NII}]\lambda 6583/\text{H}\alpha$ of ~ 2.4 and ~ 1.4 respectively, in accord to values found previously (Phillips et al., 1984, Schommer et al., 1988, Ho, Filippenko & Sargent 1997b). These galaxies are classified as Seyfert 2 galaxies with physical characteristics that account for the ratio observed in the nucleus (Kennicutt, Keel & Blaha 1989, Ho, Filippenko & Sargent 1997a, Ho, Filippenko & Sargent 1997b).

3.2.2. $[\text{SII}]/\text{H}\alpha$ and $[\text{SII}]\lambda 6716/[\text{SII}]\lambda 6731$

The ratio of $[\text{SII}]/\text{H}\alpha$ is found in the range from 0.07 to 0.2 with no obvious difference in either side of circumnuclear regions. It is in the range from 0.1 to 0.3 from the compact nucleus in galaxies with circumnuclear structures and it is 0.1 to 0.4 in central regions of galaxies without circumnuclear regions (see Tables 2 and 3). The lower values seem to be from the eastern and western side of the nuclei, but further observations with longer integration times and wider slits are needed to confirm this. Ratios with larger values from nuclei and low values from circumnuclear regions have been found in NGC 1097 (Phillips et al., 1984) and NGC 5728 (Schommer et al., 1988).

The $[\text{SII}]\lambda 6716/[\text{SII}]\lambda 6731$ ratio was found to be in the interval from 0.6 to 1.4, suggesting electron densities of a few hundred particles per cm^3 (see Tables 4 and 5; e.g. Osterbrock 1989).

4. Summary

We have presented new long slit spectroscopic observations with $[\text{NII}]$, $\text{H}\alpha$ and $[\text{SII}]$ emission lines from 18 RSA barred spiral galaxies, eight of which have structures around the nucleus. The main results are the following: a) We were able to determine the heliocentric optical velocities for the ionized gas from the compact nucleus, and the eastern and western regions, in eight galaxies. With these velocities we have estimated the inner dynamical mass of each galaxy assuming that the gas move in circular orbits on the plane of the galaxy. b) We were able to estimate the line ratios $[\text{NII}]\lambda 6548/\text{H}\alpha$, $[\text{NII}]\lambda 6583/\text{H}\alpha$, $[\text{SII}]\lambda 6716/\text{H}\alpha$ and $[\text{SII}]\lambda 6730/\text{H}\alpha$ for the eastern, western, and compact nuclear regions, separately, of eight galaxies. In particular, we found that in galax-

ies with clear circumnuclear rings, as in NGC 4314 and NGC 6951, the ratio $[\text{NII}]\lambda 6583/\text{H}\alpha$ is lower in the eastern region than in the western region of the ring suggesting different local physical conditions as a result of star formation and evolution. c) In NGC 4477, NGC 5728 and NGC 6951 we found that the ratio $[\text{NII}]\lambda 6583/\text{H}\alpha$ is larger than unity in the central nuclear regions, in agreement with values reported.

Acknowledgments

We acknowledge useful comments from the referee that helped us to improve the final version of this paper. J.A.G-B acknowledges partial financial support from DGAPA (UNAM) and CONACYT (971010), México, that allowed him to spend his sabbatical year at the Astronomy Department of the University of Minnesota and he would like to thank the Astronomy Department of the University of Minnesota for their hospitality where part of the original article was written. H.A. thanks the Spanish Ministry of Foreign Affairs for financial support. J.F. acknowledges the support given to this project by DGAPA-UNAM grant, CONACYT grants 400354-5-4843E and 400354-5-0639PE, and a R&D Cray research grant. This research has made use of the NASA/IPAC extragalactic database (NED) which is operated by the Jet Propulsion Laboratory, Caltech, under contract with the National Aeronautics and Space Administration.

REFERENCES

- Appenzeller, I., & Östreicher, R., 1988, *AJ*, 95, 45
- Arsenault, R., Boulesteix, J., Georgelin, Y., & Roy, J.-R. 1988, *A&A*, 200, 29
- Baldwin, J.A., Phillips, M.M., & Terlevich, R. 1981, *PASP*, 93, 5
- Barth, A.J., Ho, L.C., Filippenko, A.V. & Sargent, W.L.W. 1995, *AJ*, 110, 1009
- Benedict, G. F., Smith, B. J. & Kenney, J. D. P. 1996, *AJ*, 111, 1861
- Binney, J. & Tremaine, S. 1987, *Galactic Dynamics* (New Jersey: Princeton, Univ. Press)
- Boer, B. & Schulz, H. 1993, *A&A*, 277, 397
- Burbidge, M., & Burbidge, G.R. 1960a, *ApJ*, 132, 30
- Burbidge, M., & Burbidge, G.R. 1960b, *ApJ*, 132, 654
- Burbidge, M., & Burbidge, G.R. 1962, *ApJ*, 135, 694
- Burbidge, M., & Burbidge, G.R. 1964, *ApJ*, 140, 1445
- Burbidge, M., & Burbidge, G.R. 1965, *ApJ*, 142, 634
- Burbidge, M., Burbidge, G.R. & Prendergast, K.H. 1960, *ApJ*, 132, 661
- Buta, R. 1986, *ApJS*, 61, 639
- Buta, R. 1995, *ApJS*, 96, 39
- Buta, R., & Crocker, D. D., 1991, *AJ*, 102, 1715
- Contini, T., Wozniak, H., Considere, S.G., & Davoust, E. 1997, *A&A*, 324, 41
- Contopoulos, G., & Grosbøl, P. 1989, *A&A*, Rev. 1, 261
- Filippenko, A.V. & Sargent, W.L.W. 1985, *ApJS*, 57, 503
- Friedli, D., & Benz, W. 1993, *A&A*, 268, 65
- Garcia-Barreto, J. A., Carrillo, R., Klein, U., & Dahlem, M. 1993, *Rev.Mex.Astron.Astrof.*, 25, 31
- Garcia-Barreto, J. A., Dettmar, R.-J., Combes, F., Gerin, M., & Koribalski, B. 1991a, *Rev.Mex.Astron.Astrof.*, 22, 197
- Garcia-Barreto, J. A., Downes, D., Combes, F., Gerin, M., Magri, C., Carrasco, L., & Cruz-Gonzalez, I. 1991b, *A&A*, 244, 257
- Garcia-Barreto, J.A., Downes, D., & Huchtmeier, W.K. 1994, *A&A*, 288, 705
- Garcia-Barreto, J. A., Franco, J., Guichard, J., & Carrillo, R. 1995, *ApJ*, 451, 156
- Garcia-Barreto, J. A., Franco, J., Carrillo, R., Venegas, S. & Escalante-Ramirez, B. 1996, *Rev.Mex.Astron.Astrof.*, 32, 89
- Genzel, R., Weitzel, L., Tacconi-Garman, L.E., Blietz, M., Cameron, M., Krabbe, A., Lutz, D. & Sternberg, A. 1995, *ApJ*, 444, 129
- Heckman, T.M., Balick, B., & Crane, P.C. 1980, *A&AS*, 40, 295
- Helou, G. 1986, *ApJ*, 311, L33
- Ho, L.C., Filippenko, A.V. & Sargent, W.L.W. 1995, *ApJS*, 98, 477
- Ho, L.C., Filippenko, A.V. & Sargent, W.L.W. 1997a, *ApJ*, 487, 591

- Ho, L.C., Filippenko, A.V. & Sargent, W.L.W. 1997b, ApJS, 112, 315
- Ho, L.C., Filippenko, A.V., Sargent, W.L.W. & Peng, C.Y. 1997, ApJS, 112, 391
- Huchtemier, W.K. & Richter, O-G., 1989 *A General Catalog of HI Observations of Galaxies*, Springer Verlag, New York
- N.U. & Sandage, A.R. 1956, AJ, 61, 97
- Hummel, E., van der Hulst, J. M., & Keel, W. C. 1987, A&A, 172, 32
- Keel, W.C., 1983a, ApJ, 268, 632
- Keel, W.C., 1983b, ApJ, 269, 466
- Keel, W.C., 1983c, ApJS, 52, 229
- Kennicutt, R.C., 1992a, ApJ, 388, 310
- Kennicutt, R.C., 1992b, ApJS, 79, 255
- Kennicutt, R.C., Keel, W.C., & Blaha, C.A. 1989, AJ, 97, 1022
- Kennicutt, R. C., & Kent, S. M. 1983, AJ, 88, 1094
- Kenney, J. D. P., Wilson, C. D., Scoville, N. Z., Deveroux, N., & Young, J. S. 1992, ApJ, 395, L79
- Noguchi, M., 1988, A&A, 203, 259
- Osterbrock, D.E. 1989, *Astrophysics of Gaseous Nebulae and Active Galactic Nuclei* (Mill Valley California: University Science Books)
- Phillips, M.M., Pagel, B.E.J., Edmunds, M.G. & Diaz, A. 1984, MNRAS, 210, 701
- Pogge, R. W. 1989a, ApJS, 71, 433
- Pogge, R. W. 1989b, ApJ, 345, 730
- Sandage, A., & Tammann, G.A. 1987, *A Revised Shapley-Ames Catalog of Bright Galaxies* (Washington, D.C: Carnegie Institution of Washington)
- Schommer, R. A., Caldwell, N., Wilson, A. S., & Baldwin, J. A., 1988, ApJ, 324, 154
- Smith, B.J., Kleinmann, S.G., Huchra, J.P. & Low, F.J. 1987, ApJ, 318, 161
- Stauffer, J.R., 1982a, ApJ, 262, 66
- Stauffer, J.R., 1982b, ApJS, 50, 517
- Strauss, M.A., Huchra, J.R., Davis, M., Yahil, A., Fisher, K.B. & Tonry, J. 1992, ApJS, 83, 29
- Telesco, C. M., Dressel, L. L., & Wolstencroft, R. D. 1993, ApJ, 414, 120
- Tully, R.B. 1988, *Nearby Galaxy Catalog* (Cambridge: Cambridge Univ. Press)
- Vaceli, M.S., Viegas, S.M., Grünwald, R. & de Souza, R.E. 1997, AJ, 114, 1345
- Vila-Vilaró, B., Robinson, A., Pérez, E., Axon, D.J., Baum, S.A., González-Delgado, R.M., Pedlar, A., Pérez-Fournon, I., Perry, J.J. & Tadhunter, C.N. 1995, A&A, 302, 58
- Wiklind, T., Henkel, C., & Sage, L. J. 1993, A&A, 271, 71
- Young, J. S., Xie, S., Tacconi, L., Knezek, P., et al., 1995, ApJS, 98, 219